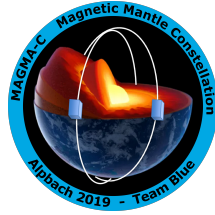


MAGMA-C Mission



MAGnetic MANTle Constellation

Team Blue: Fanny Boutier, David Byrne, Daniele Calvi, Sreemoyee Chakraborty, Marie Fayolle, Fabian Mueller, Samuel Ocaña Losada, Lidia Luque, Tatu Peltola, Alice Praet, Wolfgang Senoner, Jan Snizek, Panagiotis Trifa, Jesús Vilaboa Pérez, Sebastian Zieba, **Tutors:** Jérôme Loicq, Adriana Elizabeth Nuncio Quiroz

Date: July 24th, 2019

ABSTRACT

MAGMA-C is a proposed eight-satellite constellation in a Low-Earth Orbit (LEO) to measure Earth's magnetic field in order to study the induced magnetic field in the mantle. The primary objective of the MAGMA-C mission is to provide an unprecedented 3D conductivity profile of the Earth's mantle, derived from its induced field. The mission will measure the total magnetic field using scalar and vector field magnetometers and will separate the different magnetic field contributions in order to isolate the mantle-induced field. The major advantage of our mission is the use of a micro-satellite constellation, improving the measurement's spatial and temporal resolution compared to previous magnetic field dedicated space missions (Ørsted, CHAMP, SWARM). This directly relates to the quality of the magnetic field sources separation process, and thus to the accuracy of the extracted mantle field. Taking advantage of the higher resolution provided by the micro-satellites constellation, MAGMA-C mission aims at bringing the current knowledge of the conductivity profile of the Earth's mantle one step further, providing the first 3D conductivity profile derived from space measurements. Combined with seismic tomography measurements and laboratory experiment data, the 3D-conductivity profile delivered by the MAGMA-C mission can better constrain temperature and water content of the Earth's mantle. This will provide further insights into Earth's internal dynamic processes as well as into terrestrial planetary formation.

Keywords: mantle – electrical conductivity – 3D conductivity map – magnetic field – micro-satellite constellation

1. Introduction

Conductivity mappings of the mantle are an important technique to improve our understanding of a part of the Earth that is very difficult to directly measure. From plate tectonics and seismology to the formation of planets, conductivity mappings carry the answers to some of the most fundamental questions we have, not only about the planet we inhabit but also about the ones we will discover.

Current knowledge of the Earth's mantle conductivity is based on 1) ground-based magnetic field measurements and 2) previous space missions such as Ørsted, CHAMP and SWARM (Civet et al. 2015).

3D conductivity profiles have been obtained from a global network of ground-based magnetometers (Semenov and Kuvshinov, 2013). However, due to poor coverage, there are major discrepancies between the different models produced with these datasets (Figure 1). Clearly, doing the measurements from space greatly improves the coverage. It does, however, also lead to challenges, the main one being the separation of the magnetic signals from the ionosphere and the magnetosphere, which requires good temporal resolution. As of now, no 3D conductivity profiles have been produced with satellite data (Semenov and Kuvshinov, 2013).

Our goal is to change this. With the miniaturization of instruments and the technological maturity of small satellite constellations obtained in the last few years, it is now feasible to launch a mission that will provide the

temporal resolution needed to create a global 3D conductivity model. We propose a constellation of 8 microsattellites in four orbital planes to achieve this goal.

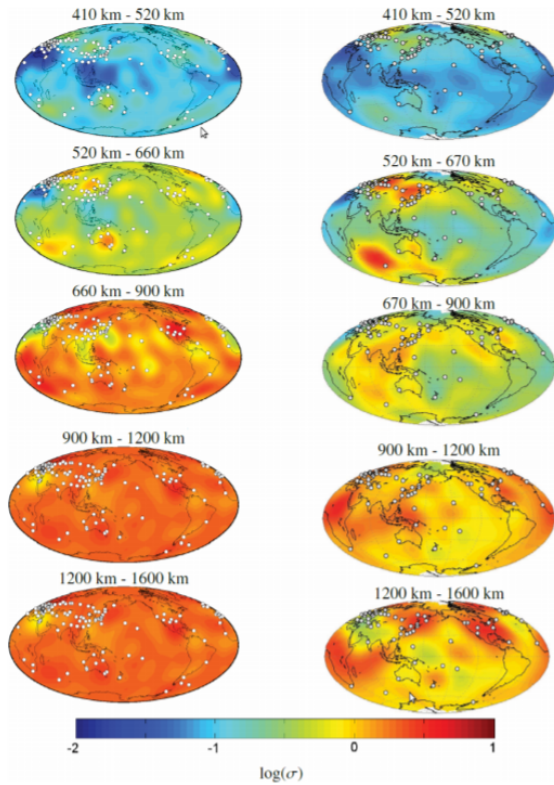


Fig. 1.: Comparison of 3D-conductivity profile derived from ground-based measurements for different depths, from Semenov and Kuvshinov, 2013 (left-hand plots) with results from Kelbert et al. (2009) (right-hand plots) (Semenov and Kushinov, 2013).

2. Science Objectives

To measure the total magnetic field at ionospheric altitudes with a high spatial and temporal resolution to isolate the magnetic field due to induced currents in the mantle.

2.1 Primary Objective

The primary aim of this mission is to establish a

global 3D conductivity profile of the mantle from the induced magnetic field due to magnetospheric and ocean currents.

2.2 Specific Objectives

The 3D conductivity mapping of the mantle can be used to infer the presence and quantity of water dissolved in the mantle. Water in the mantle is present in the form of H^+ and O^- ions (Bolfan-Casanov, 2012). The availability of charge carriers increases the conductivity of the mantle by one to two orders of magnitude given the water concentrations expected in the mantle. This increase is much larger than the change in conductivities expected from temperature or composition changes present in the mantle. Water is therefore relatively easy to detect by using conductivity profiles, even when the composition and temperature are not very well characterized.

Water is known to be present in large quantities in Earth's mantle. In fact, this dissolved water in the mantle accounts for most of the Earth's water content. It is therefore not surprising that it is a key variable in many geological processes. It is known that water weakens the structure of olivine, the main mantle component. One of the consequences of this physical change is the decrease in seismic wave speed due to the reduction in elastic stiffness associated with proton weakening. Furthermore, numerical models of lithospheric loadings indicate that this weakening is necessary to allow crust subduction, which is a key driver of plate tectonics. This knowledge on the relation between water and plate tectonics can be extrapolated to the study of other planets. NASA's Magellan spacecraft mission observed a lack of plate tectonics on Venus, which was linked to a likely absence of water in its mantle (Hirschmann, 2012).

Conductivity can also be translated, albeit more ambiguously, to temperature changes. Temperature is not as strongly related to conductivity as water is, and therefore the auxiliary data needed to make the conversion needs to be more accurate. Both composition models and laboratory measurements are needed to convert the conductivity profile into a temperature profile. Temperature is an important input in models of mantle structure and convection, and the models could therefore be better constrained by improving the temperature data provided as input.

3. Science Rationale

3.1 Earth's magnetic field contributions

The Earth's magnetic field is a superposition of the core, crustal, ocean tide, magnetospheric and ionospheric fields together with the induced mantle fields. These fields can be arranged by the typical frequencies with which they vary. The most stable field is the crustal field, which originates from magnetized material deeply embedded in the crust. The core field does, on the other hand, vary with time, albeit slowly. It originates when the dynamo action in the Earth's core moves conducting material across the weak magnetic field created by radioactive decay in the core. This creates an electric current which in turn generates a magnetic field. The addition of these two core field contributions creates a much stronger field which is tilted approximately 11° with respect to the Earth's axis of rotation. The currents in the magnetosphere and the ionosphere create magnetic fields that are highly time-dependent. The movement of seawater through Earth's magnetic field also creates a current resulting in a magnetic field contribution with a well-characterized periodicity of 12.42h (Hsieh, 1987). All these time varying magnetic field contributions induce currents in the mantle, which does not have its own intrinsic field (Love, 2008).

3.2 Selected inducing sources to map induced responses in the mantle

The different contributions to the total magnetic field that are recalled in Equation 2 can be divided into two classes: internal and external. Internal contributions are the ones originating from regions located lower than the altitude at which the spacecraft is flying (core, mantle, crust, tides, and ionospheric fields). On the other hand, external contributions refer to contributions which come from regions below the spacecraft orbit (only magnetospheric field). The key point of the contributions separation is that the induced field in the mantle is an internal field. Because induced signals have the same frequencies as the inducing signals, frequency analysis cannot distinguish between them, whereas they still to be isolated from each other for the induced signal to be captured. For this reason, only external contributions can be used as inducing signals to isolate the corresponding mantle induced signals, so that they can be separated

by calculating the gradient of the measured field with respect to the radial distance (Gauss method). Magnetospheric currents can thus be used as sources to measure the inducing response in the mantle. Additionally, the tidal field can also be used as another inducing source. Indeed, even if it is an internal source (below the spacecraft altitude), its frequency is very precisely known (12.42h) and its spatial resolution as well (defined by the oceans location), making the separation between inducing and induced fields possible even if the inducing source is internal.

In our mission, both tidal and magnetospheric fields will be used as inducing source to capture the mantle-induced response. The frequency of the tidal field is very precisely defined. On the other hand, the frequencies of the inducing signals that can be used to extract the induced field signals in the mantle are driven by the following constraints:

- Signals with $T < 1$ year to avoid overlapping with core secular variations
- Signals with $T > 1$ day as daily ionospheric variations cannot be separated from the field they induce in the mantle.

Thus, the periods of the inducing signals that can be used to extract the induced mantle field are constrained in the range **[2 day - 6months]**.

The depth at which these currents are induced, called skin depth, is a direct function of the frequencies of the inducing sources and the conductivity of the mantle.

$$\delta = \sqrt{\frac{\rho}{\pi f \mu}} \quad (1)$$

δ is the skin depth, ρ is the resistivity, f is the frequency of the inducing source and μ is the magnetic permeability (Cutnell and Johnson, 2012).

From equation (1) it follows that lower frequencies penetrate deeper into the mantle, assuming the other variables are kept equal. From the selected inducing sources, the depths down to which the mantle-induced response can be mapped are derived from the skin effect equation (Table 1).

Table.1.: Induction sources used to probe the mantle with corresponding periods and skin depths.

Source	Period	Skin depth
Magnetosphere (ring current)	2 days - 6 months	≈ 400 - 1600 km
Ocean tides	12.42hr	10-300km

3.3 Separation of the different magnetic field contributions

While flying through the ionosphere, the measured magnetic field is the total field, but the different contributions of this total field have to be separated out, in order to isolate the mantle induced field. This relationship is described in equation (2):

$$\underline{B}_{measured} = \underline{B}_{core} + \underline{B}_{crust} + \underline{B}_{tides} + \underline{B}_{magsph} + \underline{B}_{ionsph} + \underline{B}_{mantle} \quad (2)$$

The different field contributions still need to be separated, so that the induced mantle field is eventually separated out. The key requirements to perform the separation between the different contributions are:

- Removing the strong daily ionospheric variations (periods of 24, 12, 8, 6 hours...) by having 8 local times (evenly distributed) so that the local time separation is about 3 hours.
- High temporal resolution to capture the extremely short time-varying signals in the magnetospheric (required as the magnetospheric currents are the major inducing sources to map the mantle field). This will be done by having a full coverage of the Earth in one hour with a relatively low spatial resolution (1000s of km) and a higher spatial resolution (100s of km) after 1 day.
- The rest of the contributions (crust, core, tidal fields) are much more straightforward to remove because they are static or show very slow variations (crust and core fields respectively) or because their frequency and spatial resolution are well-defined (tidal field).

Additionally, because the ionospheric field can show very localised variations, a Langmuir probe (measuring electron density and temperature) will be used to flag epochs with high magnetic activity.

Combining the measurements of the total magnetic field with the current position of the satellites we will be able to get the calibrated magnetic vector field data with respect to the geophysical frame. Using auxiliary data from ground-based measurements by magnetometers and ionosondes we will create a model of the ionospheric contributions. Comprehensive inversion (Sabaka et al. 2013) will be used to separate the field sources with the help of models describing the characteristics of each source. Known sources, such as the static crustal field as measured by SWARM, are included in the model to aid the separation. The results of comprehensive inversion will be the spherical harmonic coefficients describing the internal field from the mantle and the external source field. These will be used to obtain the C-responses (Olsen 1998) describing the response of the mantle to external fields as a function of frequency. Following this procedure and applying a Bayesian inversion process we will finally derive a 3D map of mantle conductivity.

3.4 Summary of the science Requirements

The scientific requirements have been summarized in Table 2.

Table.2.: Summary of the main scientific and derived mission requirements of MAGMA-C.

Scientific Requirements	Mission Requirements
Measure day-nightside ionosphere variations.	min 8 different local times evenly distributed
Map irregular, quickly-varying magnetospheric currents	Coarse (~1000km) coverage of Earth in 1h
Mapping of the mantle response to magnetospheric currents	Finer (~300km) coverage of Earth in 1day
Measure ionospheric local phenomena	Altitude between 350-550 km

3.5 Data Products

MAGMA-C will aim to produce a 3D conductivity profile of the mantle, with high spatial and temporal resolution (complete coverage of the Earth, with 3 hours separation in local time, down to a spatial resolution of few 100s of km after 1 day). Once combined with laboratory experiments and seismic data, both the water content and temperature profile can be better characterised. Additionally, the current ionospheric models can be improved, by making use of the 3 hours local time separation to capture the daily variations and by flagging data when the electron densities differ too much from their nominal value.

4. Payload

The instruments required to successfully execute the scientific objectives of MAGMA-C are summarized in Table 3, and traced to the respective scientific demand.

Table 3.: Instruments onboard the MAGMA-C

Instrument	Function	Requirement	Measurement Accuracy	TRL
Vector Field Magnetometer (VFM)	To measure the magnetic field three components	Magnetic field strength: ± 25000 nT to ± 60000 nT Noise density: <1 nT/√Hz in 0-11 mHz Sample rate: 1 Hz	Range of ± 65000 nT and noise density: 25 pT/√Hz	6 (No flight heritage)
Absolute Scalar Magnetometer (ASM)	To measure absolute value of the magnetic field strength	Accuracy: 1 nT \rightarrow 0.001°	Range of ± 71428 nT and noise density: 15 pT/√Hz	6 (No flight heritage)
Star Tracker	To provide precise attitude determination of the VFM	Accuracy: 1 nT \rightarrow 0.001°	Accuracy: 2 arc seconds \rightarrow 0.0005°	6 (No flight heritage)
Langmuir Probe	To measure electron density, temperature and electric potential	Ionospheric storms range: 100Hz - 3KHz	Range of 10 Hz to 4 KHz	9 (on-board mission Astrid2)

Due to the scientific requirements, a magnetometer with a measurement range of 65000 nT is needed. Each spacecraft is equipped with a Vector Field Magnetometer (VFM) as well as an Absolute Scalar Magnetometer (ASM).

The Vector Field Magnetometer (VFM) selected is the *miniaturised fluxgate sensor LEMI-020*, which will measure the three components of the magnetic field within the range specified and a noise density of 25 pT/√Hz, developed by Lviv Center of Institute for Space Research.

Fundamental elements associated with the sensor *LEMI-020* are three identical star trackers, sold by CubeSatShop and developed by KU Leuven. They fulfil the function of monitoring the orientation of

the three measured components of the magnetic field. Three star trackers are necessary to continue interpreting magnetic field measurements in the eventuality that of one star tracker is Sun blinded. The star tracker accuracy is 0.0005° .

Simultaneously, the Absolute Scalar Magnetometer (ASM) will measure the absolute value of the magnetic field strength, independently from the magnetic field direction. This is required for performing in-flight calibration of the VFM in order to reduce offset and drift issues. The selected ASM is the rubidium isotope ^{87}Rb *miniature atomic scalar magnetometer* (Korth et al., 2016), characterized by a measurement maximum value of 71428 nT.

In complement of those three scientific instrument types, a langmuir probe will provide measurements of electron density and temperature as well as electric potential. The range of frequencies that must be obtained are between 100 Hz to 3000 Hz (Crowley and Azeem, 2018), as it is required to characterize storms which create ionospheric high-density bubbles. The monitoring of these bubbles is necessary for magnetic field measurement corrections. The selected langmuir probe is characterized by a relative electron density error of 10 %, as well as a 4000 Hz low pass filter and 10 Hz high pass filter (Holback et al., 2011).

5. Mission Profile

To meet the local time sampling requirement, a microsatellite constellation will be launched into LEO in order to probe the electrical conductivity of the mantle. MAGMA-C consists of eight replica satellites localized on four separate orbital planes, thereby yielding eight local times. This is important to increase the temporal resolution of our measurements as well as achieving the required 3° (300 km) sampling at the equator. Additionally, the satellites will be separated by 180° in the mean anomaly. Further details of the constellation and the parameters can be found in Figure 2 and Table 4.

Table 4.: Constellation orbital parameters.

Constellation	87°: 8/4/0.5
Altitude	550 km
Eccentricity	Circular
Coverage	8 evenly spaced local times & 300 km spatial

	resolution at the equator
Delta RAAN	45°

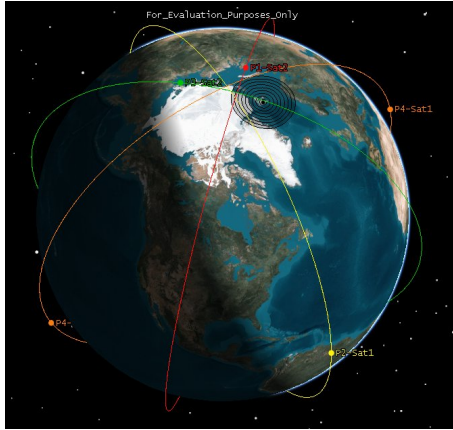


Fig. 2.: 3D model of the MAGMA-C constellation with Svalbard ground station.

5.1 Launcher

Electron launcher, provided by *Rocket Lab*, has been decided as the primary launcher. It has the capacity of deploying 150 kg into 500 km SSO. This is also the cheapest solution considering that the mass per launch is no bigger than 150 kg with an uncommon orbit, which will make difficult to find someone to share the cost of a bigger launcher. The estimated total launch cost is of 48k USD per kilogram. The selected backup launcher is the *Pegasus* rocket.

The selected launch site is the future platform in Anbøya in Norway. This European launch site was selected because of its fairly north in latitude and will provide services specialised for nano- and micro- satellites. If it is not ready by 2024, the *Rocket Lab*'s launch complex in Mahia, New Zealand, will be used.

5.2 Launch and Early Operations Phase

The initial configuration of the constellation will be achieved by two launches that will insert each group of four satellites into two quasi-polar orbits (87°), separated by 90° in Right Ascension of Ascending Node (RAAN). After achieving contact with the satellites, the multiple subsystems will be activated and monitored before performing boom deployment.

Then, the satellites will be placed in the transfer orbit in order to achieve the final configuration. Due to the fact that a change of the RAAN in the vicinity of the Earth is a high-cost manoeuvre in terms of fuel consumption, it has been decided to make use of the J_2 perturbation of the Earth to obtain this relative separation between planes. In this situation, high use of fuel has been traded-off with a transfer time of three months.

After consideration of several orbital configurations to maximise the relative motion in RAAN, a change in the inclination (2°) of the orbits was proven to be the most effective. Therefore, a pair of satellites will be inserted in an 89° inclination orbit while the other pair will be placed in an 85° orbit. A similar process will be performed for the other planes. This manoeuvre has a cost of 265 m/s per satellite and requires a precision of 1° in attitude determination. At the end of these three months, the phasing of each pair of spacecraft will be performed to obtain a difference in 180° in the mean anomaly increasing the semi-major axis of one of them. Finally, when the separation of 45° in RAAN is achieved, the satellites will be returned to the operative orbit to perform the scientific mission.

5.3 Operational life

During its operational life, the satellite will perform its mission with minor ground operations. The design allows for stabilisation by gravity gradient, and body-mounted solar panels will provide enough power, removing the need for solar pointing strategies.

A downlink strategy of eight days has been found to be optimal, in terms of the operational cost versus the on-board memory. It will be performed using one of the two low-gain antennas mounted in the nadir face of the satellite, as the latter is on Nadir looking configuration and no pointing is required. It has been decided to use Svalbard as main ground station, as it offers the longest minimum connection window for all the orbits simultaneously.

A study of the environmental disturbances has proved that most of the disturbance torques can be corrected using the reaction wheels and magnetorquers mounted on the spacecraft. The only correction of the orbit altitude is required after 5 years of operations due to atmospheric drag. It will be performed when the satellite reaches an altitude of 500 km, boosting it back to 550 km. This manoeuvre has a consumption of 27.5 m/s.

5.4 De-orbit

The satellite meets the IADC guidelines for space debris mitigation, performing a natural destructive reentry (risk assessment less than 10^{-4}) in less than 25 years after end-of-mission.

6. Spacecraft Design

Fig. 3 illustrates the arrangement of the spacecraft's subsystems and its deployed configuration.

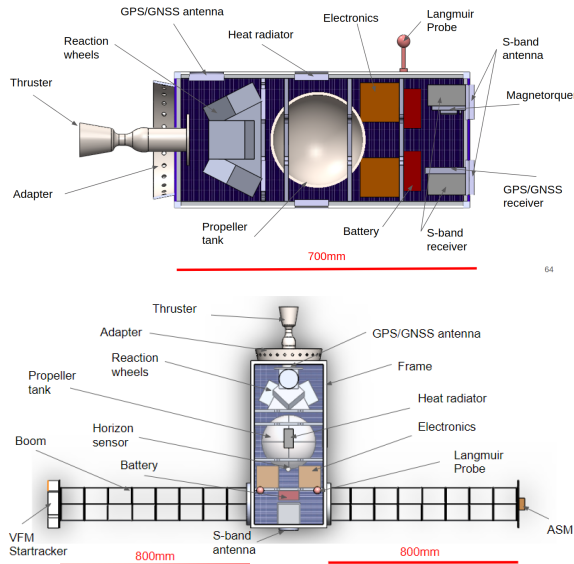


Fig. 3.: Illustrations of the spacecraft configuration.

Using the moment of inertia of spacecraft for stabilization in nadir pointing provide us with direct pointing upon the smallest area of the spacecraft to the Earth (better efficiency of solar cells, smaller power consumption, patch antenna orientation).

6.1 Structure

The primary structure of Magma-C consists of a lightweight Al-6061 symmetrical frame reinforced by a honeycomb core sandwich panel out of AlMn, which benefits from a long successful history. This symmetry counteracts the magnetic field generated by the electronics. The frame provides the major load path between the spacecraft's components and the launch vehicle. Its internal volume is designed in such a way that all mission-specific equipment is mounted properly via mounting plates. The dimensions of the spacecraft envelope excluding the

deployed booms are 340x360x935mm and 340x935x2066mm when deployed.

6.2 Mechanism

The only deployment mechanisms for a Magma-C satellite are the two booms. For this, the *Coilable Boom System* developed by *Northrop Grumman*, will be used, which benefits from a long successful heritage. Its main positive drivers are magnetic "cleanliness", excellent thermal stability, a low mass and a compact mast stowage.

6.3 Propulsion System

A single monopropellant thruster will be used for the orbit manoeuvring. In order to perform the manoeuvre in one orbit, the *22N High Performance Green Propulsion (HPGP) Thruster* developed by *Bradford ECAPs* (Bradford Ecaps website page) was chosen. This 25W thruster can provide 22 N of thrust, 243 s of specific impulse and weighs 1.1 kg. The propellant will be stored in a spherical tank with a radius of 113 mm as it provides the smallest surface-to-volume ratio in comparison to other tank geometries, and the minimum wall thickness for a given internal pressure (Huzel and Huang, 1971). It is composed out of Al-6066-T6.

6.4 Attitude Orbit and Control System

The Nadir looking Magma-C spacecraft is stabilized via three-axis control using four reaction utilizing actuators. Three reaction wheels are mounted on separate orthogonal planes and one wheel is used for redundancy. Three magnetic torquers are implemented for producing torques proportional and perpendicular to the Earth's magnetic field at lower orbits. With regards to the sensors selection, a GPS device including a patch antenna ensures high accuracy in locating and navigating the spacecraft. Concerning the stabilization of the spacecraft an IMU is also implemented. It consists of three gyroscopes and 3 accelerometers for the calculation of the external forces affecting the spacecraft. Finally, a pair of horizon sensors is selected for providing Earth-related information to the spacecraft, ensuring improved performance and redundancy at the same time

For three-axis attitude stabilisation, the *NanoTorque GSW-600* manufactured by *GOMspace*, which is a four wheel redundant setup

6.5 Thermal Control

The battery packs and the propulsion system will be equipped with heaters. The radiators with an

approximate area of 0.02 square meters will emit about 4.8W. The propellant tank is coated with multilayer insulation. The minimum equilibrium temperature is at -53.4°C and maximal at 55.5°C.

6.6 Power

Two packs of batteries with a capacity of 77 Wh and 8 cells each for energy storage will be used. The surface of a spacecraft will be covered by solar panels with a total area of 0.7 m² except for the Nadir nozzle face. This assumes that the reaction wheels will not be switched on all the time. A summary of the power budget for each operating mode is presented in Table 5.

Table.5.: Summary of the power budget for each operating mode.

Power Budget for each operating mode					
Subsystem	Safe Mode	Orbital Control Mode	Normal / Burst Mode	Commissioning Mode	Downlink Mode
Science Instruments	-	-	4.5 W	-	-
Telecommunication	2 W	2 W	2 W	2 W	8 W
Propulsion	-	8 W	-	-	-
C&DH	5 W	5 W	5 W	5 W	5 W
ADCS	-	30.5 W	30.5 W	30.5 W	30.5 W
Structure	-	-	-	10 W	-
Battery	-	-	25 W	-	-
Subtotal	7 W	45.5 W	67 W	47.5 W	43.5 W
Margin	20 %	20 %	20 %	20 %	20 %
Total	8.4 W	54.6 W	80.4 W	57 W	52.2 W

6.7 Telemetry and Telecommunications

Each MAGMA-C satellite will fly two omnidirectional low-gain S-band antennas and two transceivers manufactured by SSTL. Due to the LEO, the low-gain antennas will provide sufficient telemetry rate with low power consumption. Science data downlink will occur every eight days while housekeeping status will be communicated every day. The preferred main station is Svalbard. Data budget is presented in Table 6.

The mission will last at least five years, but it is preferred that it continues to ten years.

10. Cost Analysis

The total cost of the MAGMA-C mission has been estimated based on back-of-the-envelope calculations perusal of similar Earth-based observation missions of the past and with a contingency of 20%. Similarity indicators of interest included the number of satellites, mass and mission lifetime. To this end, NASA's CYGNSS Small Satellite Constellation, which uses

Table.6.: Data Budget for MAGMA-C.

Data Budget for each operating mode					
Type of Data	Safe Mode	Orbital Control Mode	Normal / Burst Mode	Commissioning Mode	Downlink Mode
Science Instruments	-	-	0.1 to 7.6 kbits/s	-	-
Housekeeping	-	10 kbits/s	10 kbits/s	10 kbits/s	10 kbits/s
Downlink duration	-	4.85 min	4.8 to 8.45 min	4.85 min	4.85 min

7. On-board computer

The on-board computer called *DH-MS01 Sirius C&DH* is developed by *ÁAC Microtec*. It has a 32 GB mass storage capacity and modular design approach that enables easy customization.

8. Mass Budget

The Table 7 summarizes the mass budget for the MAGMA-C mission. A margin of 20% was considered as part of this Phase 0 study.

Table.7.: Mass Budget for MAGMA-C.

Mass Budget			
Subsystem	Mass	Contingency	Total Mass
Science Instruments	2.55 kg	20 %	3.06 kg
Telecommunication	0.81 kg	20 %	0.97 kg
Propulsion	1.9 kg	20 %	2.28 kg
C&DH	2 kg	20 %	2.4 kg
ADCS	3.2 kg	20 %	3.84 kg
Structure	7.25 kg	20 %	8.7 kg
Power	5.5 kg	20 %	6.6 kg
Total Dry Mass	23.21 kg	20 %	29 kg
Harness	1.84 kg	20 %	2.2 kg
Propellant	10 kg	20 %	12 kg
Total	35 kg	20 %	42 kg

9. Mission duration

scatterometry to observe wind fields, was used as a comparison. It is also an eight-satellite constellation of similar mass per unit - approximately 24 kg - and with a mission lifetime of ~11 years and cost of 150 million USD (Ruf et al., 2018). The estimate assumed the same cost for development for each satellite, even though the satellites are of the same design and the cost is lower for subsequent development (Table 7).

Table.7.: Cost Breakdown.

Component	Cost [M€]	Notes
Satellites	80	Per unit: 10 M€ (x8)
Launcher	10	2 Launchers with max. 4 satellites each
Ground Segment	25	2.3M€ per year & 10.5 years
Project Team	35	Commissioning & operations
Total	150	-
Incl. 20% margin	180	-

11.1 Descoping Options

In this section, descoping scenarios are considered.

11.1.1 In case of boom deployment malfunction

If the boom fails to deploy, the spacecraft operations will not be interrupted. However, the magnetometer measurements will be influenced by its proximity to the onboard electronics. This will degrade the quality of the data, but measurements can still be taken.

11.1.2 In case of a launch failure

The MAGMA-C mission will start with two launches, each carrying four satellites. If one of the launches fails, the science capability may be diminished. It is important to have evenly-spaced distribution to acquire good spatial coverage. When the four satellites are deployed, they may not be evenly spaced, which would not meet the mission objectives.

However, MAGMA-C can still improve the current model for ionospheric currents, thereby delivering a byproduct of its objective.

11.2 Risk Analysis

To prevent a space mission from failure, a risk assessment is necessary. Usually, risk management is an iterative process consistently performed throughout the mission lifetime, as different risks can occur at different times. The whole risk scale is evaluated. In Table 8, red and orange rectangles indicating high to very high risk which is unacceptable in every case. Yellow indicates medium to low risk, followed by green, which reveals an acceptable risk. To identify potential risks different tasks need to be considered. Therefore different information sources are used, as the risk analysis of previous missions, simulations, test data, amongst others.

Severity	5		Scientific sensors Telecommunication			
	4	Launch stage On-board Computer	Power system			
	3		Boom deployment	AOCS		
	2			Propulsion		
	1			Orbit insertion		
		A	B	C	D	E
		Likelihood				

Table 8.: Subsystem Risk Assessment. Likelihood goes from A = acceptable to E = unacceptable, Severity varies from 1 to 5.

The key risks lie in two aspects - the first is the failure of the scientific sensors, which is far outside the acceptable risk (green) zone.

Since this is a science mission, the failure of the science sensors would render the mission unachievable. This is not likely to occur as most of the sensors are TRL 6 (tested in a relevant environment) or above. However, the VFM and ASM do not have flight heritage that presents as a source of risk. In order to mitigate the risk further, it is important to ensure that sufficient testing is done. The second risk to discuss is a failure in telecommunication presented as a high-severity, but low-likelihood event. In order to margin the possibility of a complete telecommunication failure, a second pair of S-Band Transceiver is added as well as a second low-gain antenna. This reduces the risk of a complete telecommunication failure significantly. Figure 6 is showing a preliminary risk assessment matrix, performed to identify key risks in the MAGMA-C mission.

12. Programmatic Considerations

MAGMA-C will be launched in 2024 and will have a lifetime of at least 10 years. A mission schedule is shown in Figure 7.

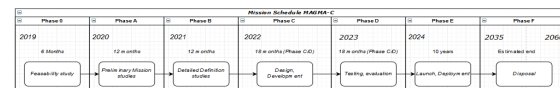


Fig. 7.: Mission schedule.

13. Public Outreach Plan

The public outreach is an underestimated component of space missions. The goal is to inform the public as well as the scientific community. MAGMA-C will have a dedicated page on several social media platforms such as Facebook or Instagram to inform the broad public of the mission milestones and accomplishments. Mission mascot drawing contests could be held in primary and/or middle schools to draw the best mission mascot for MAGMA-C.

Material explaining the scientific concept and goal of the mission understandable to primary and middle school students will be created and put online. Presentation in school classes by the PhD students will be promoted as part of their PhD outreach activities.

14. Conclusion

The MAGMA-C will perform unprecedented science by mapping the mantle conductivity in 3D, enabling insights into the mantle water content, which is critical for understanding earthquakes. An advantageous by-product of this mission would be to improve existing models of the ionosphere. Taking advantage of the technology maturity of satellite constellations and the miniaturisation of electronics, MAGMA-C will use Commercial-Off-The-Shelf (COTS) components to deliver a low-cost, low-risk and feasible mission. With this, MAGMA-C will become part of a rich history of other missions probing the deep interior of the Earth.

15. References

- Civet, F., E. Thébault, O. Verhoeven, B. Langlais, and D. Saturnino (2015), Electrical Conductivity of the Earth's Mantle from the First Swarm Magnetic Field Measurements: MANTLE ELECTRICAL CONDUCTIVITY. *Geophysical Research Letters* 42 (9): 3338–46. <https://doi.org/10.1002/2015GL063397>.
- Crowley, G., Azeem, I. (2018), Chapter 23 - Extreme Ionospheric Storms and Their Effects on GPS Systems. *Extreme events in Geospace*, pp. 555-586.
- Cutnell, J. D., Kenneth W. J. (2012) *Physics*. 9th ed. Hoboken, NJ: Wiley.
- Eken, T., Plomerova, J., Vecsey, L., Babuska, V., Roberts, R., Shomali, H., Bodvarsson, R. (2012): Effects of seismic anisotropy on P-velocity tomography of the Baltic Shield, *Geophysical Journal International*, 188, 2, pp. 600-612.
- Huzel, D.K., Huang, D.H. (1971): Chapter 8 - Design of propellant tanks, *Design of Liquid Propellant Rocket Engines Second Edition*, pp. 329-349.
- Korth, H., Strohhahn, K., Tejada, F., Andreou, A. G., Kitching, J., Knappe, S., Lehtonen, S. J., London, S. M., Kafel, M. (2016): Miniature atomic scalar magnetometer for space based on the rubidium isotope ^{87}Rb , *J. Geophys. Res. Space Physics*, 121, 7870–7880, doi:10.1002/2016JA022389.
- Love, J. J. (2008) Magnetic Monitoring of Earth and Space, *Physics Today*, 61 (2), pp. 31–37. <https://doi.org/10.1063/1.2883907>.
- Olsen, N., Stolle, C. (2012): Satellite Geomagnetism. *Annual Review of Earth and Planetary Sciences*, 40, pp. 441–465. <https://doi.org/10.1146/annurev-earth-042711-105540>
- Olsen, N. (1998) The electrical conductivity of the mantle beneath Europe derived from C-responses from 3 to 720 hr, *Geophysical Journal International*, Volume 133, Issue 2, pp. 298–308.
- Ruf, C. S., Chew, C., Lang, T., Morris, M. G., Nave, K., Ridley, A., Balasubramaniam, R. (2018) : A New Paradigm in Earth Environmental Monitoring with the CYGNSS Small Satellite Constellation, *Scientific Reports*, Volume 8, Article number: 8782.
- Sabaka, T.J., Tøffner-Clausen, L. & Olsen, N. (2013). Use of the Comprehensive Inversion method for Swarm satellite data analysis. *Earth Planet Sp*
- Semenov, A. & Kuvshinov, A. (2012). "Global 3-D imaging of mantle conductivity based on inversion of observatory C-responses—II. Data analysis and results" *Geophys. J. Int.*
- Heinson, Graham, and Steven Constable. 1992. "The Electrical Conductivity of the Oceanic Upper Mantle." *Geophysical Journal International* 110 (1): 159–79. <https://doi.org/10.1111/j.1365-246X.1992.tb00719.x>.
- Bolfan-Casanova, Nathalie, Manuel Muñoz, Catherine McCammon, Etienne Deloule, Anais Férot, Sylvie Demouchy, Lydéric France, Denis Andraut, and Sakura Pascarelli. 2012. "Ferric Iron and Water Incorporation in Wadsleyite under Hydrous and Oxidizing Conditions: A XANES, Mössbauer, and SIMS Study." *American Mineralogist* 97 (8–9): 1483–93. <https://doi.org/10.2138/am.2012.3869>.
- Hirschmann, Marc, and David Kohlstedt. 2012. "Water in Earth's Mantle." *Physics Today* 65 (3): 40–45. <https://doi.org/10.1063/PT.3.1476>.